NH_2-terminal Inactivation Peptide Binding to C-type–inactivated Kv Channels

Harley T. Kurata, Zhuren Wang, and David Fedida

Department of Physiology, University of British Columbia, Vancouver, British Columbia V6T 1Z3, Canada

ABSTRACT In many voltage-gated K^+ channels, N-type inactivation significantly accelerates the onset of C-type inactivation, but effects on recovery from inactivation are small or absent. We have exploited the Na^+ permeability of C-type–inactivated K^+ channels to characterize a strong interaction between the inactivation peptide of Kv1.4 and the C-type–inactivated state of Kv1.4 and Kv1.5. The presence of the Kv1.4 inactivation peptide results in a slower decay of the Na^+ tail currents normally observed through C-type–inactivated channels, an effective blockade of the peak Na^+ tail current, and also a delay of the peak tail current. These effects are mimicked by addition of quaternary ammonium ions to the pipette-filling solution. These observations support a common mechanism of action of the inactivation peptide and intracellular quaternary ammonium ions, and also demonstrate that the Kv channel inner vestibule is cytosolically exposed before and after the onset of C-type inactivation. We have also examined the process of N-type inactivation under conditions where C-type inactivation is removed, to compare the interaction of the inactivation peptide with open and C-type–inactivated channels. In C-type–deficient forms of Kv1.4 or Kv1.5 channels, the Kv1.4 inactivation ball behaves like an open channel blocker, and the resultant slowing of deactivation tail currents is considerably weaker than observed in C-type–inactivated channels. We present a kinetic model that duplicates the effects of the inactivation peptide on the slow Na^+ tail of C-type–inactivated channels. Stable binding between the inactivation peptide and the C-type–inactivated state results in slower current decay, and a reduction of the Na^+ tail current magnitude, due to slower transition of channels through the Na^+-permeable states traversed during recovery from inactivation.

KEY WORDS: potassium channel • Kv1.4 • Kv1.5 • inactivation • quaternary ammonium

INTRODUCTION

Inactivation of voltage-gated potassium (Kv) channels occurs by at least two broad mechanisms referred to as N- and C-type inactivation (Hoshi et al., 1990, 1991; Baukrowitz and Yellen, 1995). In channels capable of N-type inactivation, such as Kv1.4, the NH_2 terminus acts as a tethered open-state blocker, causing rapid inactivation of these channels upon opening (Choi et al., 1991; Demo and Yellen, 1991; Hoshi et al., 1991). The amino terminus of a single subunit is thought to enter and occlude the central cavity of the channel as an extended peptide (MacKinnon et al., 1993; Zhou et al., 2001). Occlusion of the inner pore by the inactivation peptide or a quaternary ammonium ion results in delayed channel closing and a pronounced immobilization of gating charge upon repolarization (Bezanilla et al., 1991; Choi et al., 1991; Demo and Yellen, 1991; Roux et al., 1998). Most other Kv1 channels, including Kv1.5, lack an NH_2-terminal inactivation ball and inactivate exclusively by a C-type inactivation mechanism (Panyi et al., 1995; Fedida et al., 1999). The conformational changes associated with C-type inactivation involve a cooperative constriction of the outer mouth of the channel pore after evacuation of K^+ ions from the permeation pathway, and can be slowed by a number of point mutations in the channel's external mouth (Lopez-Barneo et al., 1993; Yellen et al., 1994; Ogielska et al., 1995). One recent study has also suggested that C-type inactivation also causes a constriction of the intracellular aqueous cavity of Kv channels (Jiang et al., 2003a).

It is well known that N- and C-type inactivation mechanisms are not mutually exclusive. In fact, these mechanisms clearly coexist and show synergism in voltage-gated K^+ channels (Baukrowitz and Yellen, 1995, 1996; Rasmusson et al., 1995). Specifically, the onset of N-type inactivation significantly speeds the onset of C-type inactivation, demonstrated by both characterization of recovery from channel inactivation (Baukrowitz and Yellen, 1995; Rasmusson et al., 1995) and direct fluorescent visualization of conformational changes in the channel pore (Loots and Isacoff, 1998). The physiological importance of this acceleration of C-type inactivation becomes apparent during recovery from inactivation, where recovery from the C-type–inactivated state becomes a limiting process (Rasmusson et al., 1995).

The online version of this article contains supplemental material.

Address correspondence to David Fedida, Department of Physiology, University of British Columbia, 2146 Health Sciences Mall, Vancouver, BC V6T 1Z3, Canada. Tel.: (604) 822-5806; email: fedida@interchange.ubc.ca

The dynamics of inactivation peptide binding to the open state have been well characterized in several studies using experimental conditions that minimize C-type inactivation (high extracellular K^+, or pore mutations). In these experiments, unbinding of the inactivation peptide allows ions to permeate open channels, resulting in a "recovery tail" current (Demo and Yellen, 1991; Ruppersberg et al., 1991). However, C-type inactivation renders the pore of Kv channels impermeant to K^+ ions, which impedes the study of binding of the inactivation peptide or other intracellular blockers to states apart from the open state.

In this study, we have exploited the unique properties of Na^+ permeation of Kv channels, particularly the significant Na^+ permeability of C-type–inactivated Kv channels (Starkus et al., 1997; Kiss et al., 1999; Wang et al., 2000), to investigate the interactions of the inactivation peptide and quaternary ammonium blockers with the inner pore after the onset of C-type inactivation. We demonstrate that the inactivation peptide and quaternary ammonium ions exert dramatic effects on Na^+ currents through both open and C-type–inactivated channels. The observations demonstrate that open and C-type–inactivated states form patent receptor sites for the inactivation peptide, suggesting that the inner vestibule of Kv channels remains cytosolically accessible before and after the onset of C-type inactivation. We have also constructed a kinetic model that simulates the influence of the inactivation peptide on the gating of C-type–inactivated channels, and suggests that the inactivation peptide may bind the C-type–inactivated state with greater affinity than the open state.

MATERIALS AND METHODS

Cell Preparation and Transfection

Unless otherwise stated, experiments were performed on transiently transfected HEK 293 cells grown in MEM with 10% fetal bovine serum, at 37°C in an air/5% CO_2 incubator. 1 d before transfection, cells were plated with 20–30% confluence on sterile glass coverslips in 25-mm Petri dishes. On the day of transfection, cells were washed once with MEM with 10% fetal bovine serum. To identify the transfected cells efficiently, channel DNA was cotransfected with the vector pGFP (encoding a GFP protein). Channel DNA was incubated with pGFP (1 μg of pGFP, 1–3 μg of channel DNA) and 4 μl of LipofectAMINE 2000 (Invitrogen) in 100 μl of serum-free media, then added to the dishes containing HEK 293 cells in 1 ml of MEM with 10% fetal bovine serum. Cells were incubated overnight before recording, and transfected cells were identified by visualization of GFP with a standard epifluorescence microscope.

Solutions

For recordings in K^+ conditions, patch pipettes contained (in mM): NaCl, 5; KCl, 135; Na_2ATP, 4; GTP, 0.1; $MgCl_2$, 1; EGTA, 5; HEPES, 10; and the filling solution was adjusted to pH 7.2 with KOH. The bath solution contained (in mM): NaCl, 135; KCl, 5; HEPES, 10; sodium acetate, 2.8; $MgCl_2$, 1; $CaCl_2$, 1; and the solution was adjusted to pH 7.4 with NaOH. For recordings in Na^+ conditions, patch pipettes contained (in mM): NaCl, 135; Na_2ATP, 4; GTP, 0.1; $MgCl_2$, 1; EGTA, 10; HEPES, 5; and the solution was adjusted to pH 7.2 with NaOH. Na^+ bath solution contained (in mM): NaCl, 135; HEPES, 10; dextrose, 10; $MgCl_2$, 1; $CaCl_2$, 1; and the solution was adjusted to pH 7.4 with NaOH. All chemicals were from Sigma-Aldrich.

Electrophysiological Procedures

Coverslips containing cells were removed from the incubator before experiments and placed in a superfusion chamber (volume 250 μl) containing the control bath solution at ambient temperature (22–23°C) and perfused with bathing solution throughout the experiments. Whole-cell current recording and data analysis were done using an Axopatch 200A amplifier and pClamp 8 software (Axon Instruments, Inc.). Patch electrodes were fabricated using thin-walled borosilicate glass (World Precision Instruments). Electrodes had resistances of 1–3 MΩ when filled with control-filling solution. Capacity compensation and 80% series resistance compensation were used in all whole-cell recordings. No leak subtraction was used when recording currents, as very little leak was observed in our recordings. Since the channels employed in this study are closed at negative holding potentials, any residual current at the holding potential will be due to leak. In addition, cells are quite fragile during recordings in Na^+ conditions, and cannot withstand the hyperpolarizing voltage steps required for P/n leak subtraction. Data were sampled at 10–20 kHz and filtered at 5–10 kHz. Membrane potentials have not been corrected for small junctional potentials between bath and pipette solutions. Throughout the text data are presented as mean ± SE.

Molecular Biology and Channel Mutations

The mammalian expression vector pcDNA3 was used for expression of all channel constructs used in this study. All primers used were synthesized by Sigma Genosys. All constructs were sequenced to check for errors during PCR amplification.

Site-directed mutagenesis of Kv1.4 and Kv1.5 was performed using the Stratagene Quikchange kit. For preparation of the Kv1.5R487V mutant, the primers used were GGGCTGCGCTTTGCGGCGGCAGCTGGGCACCCTG and its complement. For preparation of Kv1.4 K533V, the primers used were GGGCTATGGGGACATGGTGCCCATCACTGTAGGG and its complement. The Kv1.4N/Kv1.5 chimeric construct was generated by PCR amplification of the Kv1.4 NH_2 terminus using the T7 primer and GGAATTCTCCGGATATTCAAAGAGGAGC, followed by subcloning of the fragment into a pcDNA3 Kv1.5 vector using HindIII and BspEI restriction sites.

Kinetic Modeling

The kinetic modeling and current simulations presented in this manuscript were completed using ScoP (version 3.51; Simulation Resources) and based on two previously published models of Kv1.5 inactivation (Kurata et al., 2001; Zhang et al., 2003). The number of channels moving between different states was described by a series of first-order differential equations. The transition rates between horizontal states were exponential functions of voltage of the form: rate = $k_{0mV} \cdot \exp[z_i \cdot e_0 \cdot V/kT]$, where k_{0mV} represents the rate at 0 mV, z_i refers to the valency for the transition, and e_0, V, k, and T have their usual meanings.

Online Supplemental Material

We have included an online supplement containing some additional experimental data and more in-depth consideration of the

models presented in the primary manuscript. The supplemental figure available online illustrates an additional experiment exploring binding of the inactivation peptide to the R state of our kinetic model (Fig. S1), and explores two possible expansions of our model scheme (Schemes S1 and S2). Online supplemental material is available at http://www.jgp.org/cgi/content/full/jgp.200308956/DC1.

RESULTS

Multiple Mechanisms of K^+ Channel Inactivation

We have used a double pulse protocol to illustrate the inactivation and recovery phenotype characteristic of WT Kv1.4 channel currents in Fig. 1 A. From a holding potential of −100 mV, cells were pulsed to +60 mV for 4 s to observe inactivation, repolarized to −100 mV for a variable recovery period, and pulsed again to +60 mV to determine channel availability after the recovery period. In WT Kv1.4 channels stably expressed in HEK 293 cells, we observed very rapid current decay due to N-type inactivation (Fig. 1 A). The time constant of N-type inactivation was consistently between 15–20 ms (Fig. 1 A), which is in agreement with previous studies of Kv1.4 inactivation (Rasmusson et al., 1995). Cells stably expressing a NH_2 terminally deleted form of Kv1.4ΔN147 were subjected to an identical protocol in Fig. 1 B. Deletion of the NH_2 terminus ablates N-type inactivation, and reveals the far slower process of C-type inactivation.

As mentioned, N- and C-type inactivation are not mutually exclusive, and both are known to coexist in channels such as Kv1.4 and *Shaker*. Specifically, the onset of N-type inactivation is thought to accelerate the rate of C-type inactivation, such that C-type inactivate channels shortly after binding of the NH_2-terminal ball. As a result, the full-length and NH_2 terminally truncated forms of Kv1.4 recover from inactivation at the same rate despite a 100-fold difference in their respective rates of inactivation (Fig. 1 C) (Rasmusson et al., 1995). We measured indistinguishable time constants of recovery of 4.7 ± 0.2 s (n = 10) in Kv1.4, and 4.4 ± 0.3 s (n = 8) in Kv1.4ΔN147 (Fig. 1 C).

Inactivation and Recovery in Na^+ Conditions

We have also examined the effects of the Kv1.4 inactivation peptide on inactivation and recovery after substitution of all intracellular and extracellular K^+ ions with

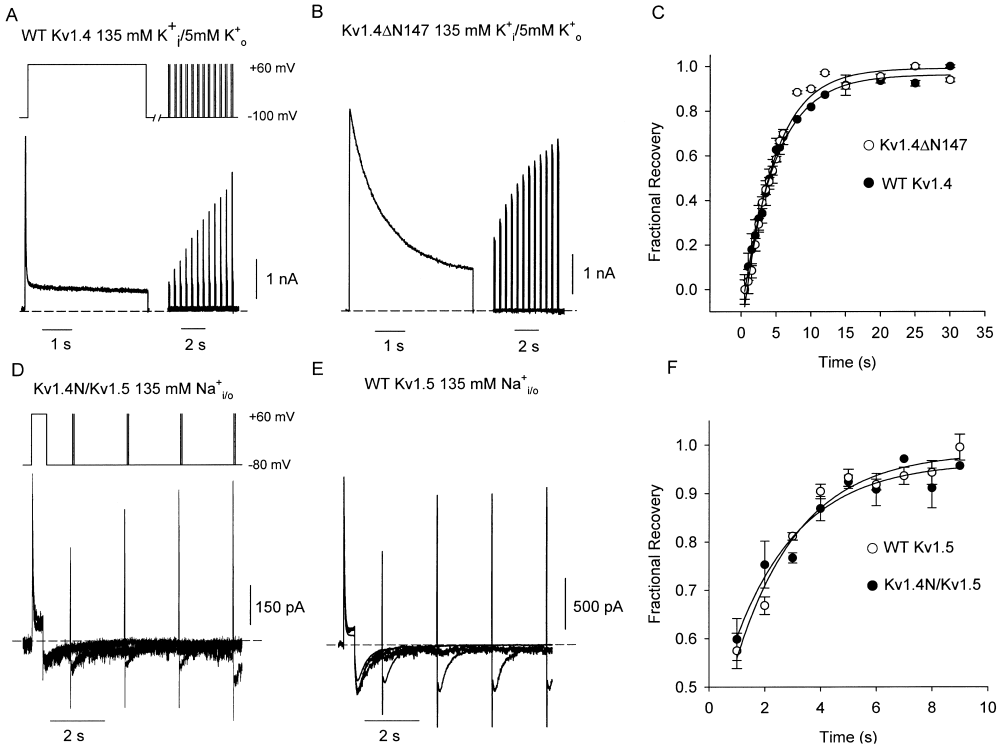

FIGURE 1. Mechanisms of N- and C-type inactivation in K^+ and Na^+ recording conditions. Currents were recorded from HEK293 cells expressing (A) WT Kv1.4 or (B) Kv1.4ΔN147 in 5 mM K^+_o/135 mM K^+_i recording conditions, using a double-pulse protocol. Cells were depolarized for 4 s to +60 mV to inactivate the channels, and cells were repolarized to −100 mV for a variable recovery period and briefly pulsed to +60 to measure recovery from inactivation. The different rates of inactivation during the 4-s depolarizing pulse reflect the presence (A) or absence (B) of N-type inactivation. The fractional recovery from inactivation is plotted against the recovery interval (C), and data points are fitted with a single exponential recovery equation. The time constants of recovery from inactivation were indistinguishable between the two constructs, measured as 4.7 ± 0.2 s in WT Kv1.4 (n = 10, ●) and 4.4 ± 0.3 s in Kv1.4ΔN147 (n = 8, ○). To measure inactivation and recovery in symmetrical Na^+ conditions, currents were recorded from HEK293 cells expressing (D) Kv1.4N/Kv1.5 chimeric channels or (B) WT Kv1.5 channels. Cells were depolarized for 400 ms to +60 mV to inactivate the channels, followed by a variable recovery period at −80 mV and a brief pulse to +60 mV to measure recovery from inactivation. The fractional recovery from inactivation is plotted against the recovery interval (F), and recovery time constants were measured as 2.35 ± 0.4 s in Kv1.4N/Kv1.5 (n = 3–5 per data point, ●) and 2.29 ± 0.3 s in WT Kv1.5 (n = 3–8 per data point, ○). As in K^+ conditions, the time course of recovery from inactivation is indistinguishable in the presence or absence of the inactivation peptide.

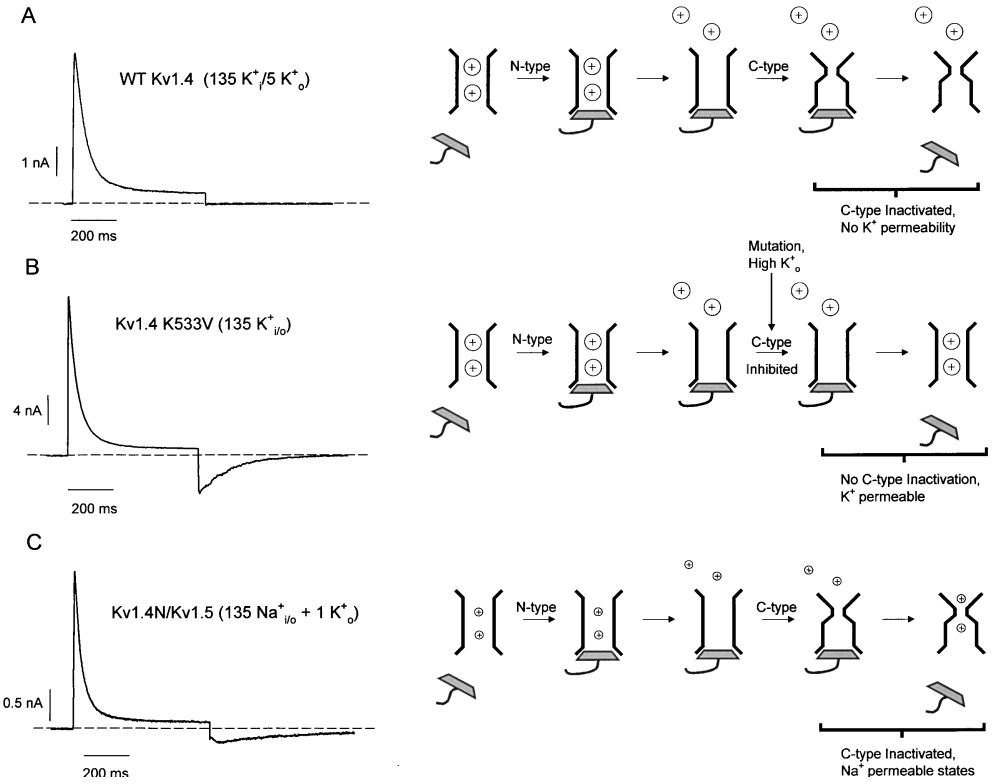

FIGURE 2. Two types of recovery tails through Kv channels. (A) Sample trace of ionic currents through WT Kv1.4 channels, in low external K^+ conditions. The schematic diagram in A demonstrates that in these ionic conditions, N-type inactivation promotes C-type inactivation, and precludes the observation of ionic tail currents upon repolarization. A sample recording of recovery tails in high K^+ conditions is depicted in B. The schematic diagram in B shows that these experimental manipulations prevent the pore constriction of C-type inactivation, and permit the observation of K^+ recovery tail currents as the inactivation peptide unbinds from the open state of the channel. The schematic diagram in C shows that if the K^+ concentration is sufficiently low, C-type–inactivated Kv channels exhibit a significant permeability to Na^+, and this permeability persists during early stages of recovery from inactivation (labeled Na^+-permeable states). This persistent Na^+ permeability results in recovery tails through C-type–inactivated channels, and thereby allows for the observation of the influence of the inactivation peptide on the kinetics of the C-type–inactivated recovery tail. A representative current trace of the recovery tails through the Kv1.4N/Kv1.5 chimeric channel (exhibits both N- and C-type inactivation) is depicted in C. In all sample traces, HEK 293 cells expressing the noted construct were depolarized to +60 mV for 600 ms, and repolarized to −100 mV to elicit tail currents.

Na^+ ions. To perform these experiments, we used a chimeric construct (Kv1.4N/Kv1.5) consisting of the NH_2 terminus of Kv1.4 fused to the channel core of Kv1.5. This experimental manipulation was necessary because WT Kv1.4 channels C-type inactivate extremely rapidly (or are closed-state inactivated) when the extracellular K^+ concentration is low, which precludes the observation of any outward current (Pardo et al., 1992). From a holding potential of −80 mV, HEK 293 cells expressing either Kv1.4N/Kv1.5 or WT Kv1.5 (Fig. 1, D and E) were pulsed to +60 mV for 400 ms, repolarized to a recovery potential of −80 mV for a variable duration, and pulsed briefly to +60 mV to determine channel availability after the recovery period. For clarity, we point out that the tail currents in Fig. 1, D and E, often appear to be accompanied by a rapid transient that can be mistaken for uncompensated capacity current. These rapid transients actually correspond to deactivation of open Kv1.5 channels, and are observed because the test pulses employed in Fig. 1, D and E, are not sufficiently long to completely inactivate the channels. Thus, upon repolarization, there are two components to the tail current: a rapid component corresponding to deactivation of channels that remained open during the test pulse, and a slow "hooked" component corresponding to channels that C-type inactivate during the test pulse. When longer depolarizations are employed (in later figures), C-type inactivation is essentially complete, and the rapid component of the tail current disappears. This biphasic nature of the Na^+ tail has been carefully characterized in a previous publication (Wang et al., 2000).

As in K^+ conditions, the rates of recovery from inactivation in the presence or absence of the inactivation peptide are very similar (Fig. 1 F). We measured time constants of recovery of 2.4 ± 0.4 s in Kv1.4N/1.5, and 2.3 ± 0.3 s in WT Kv1.5. Importantly, these experimental conditions differ from those depicted in Fig. 1, A–C, because they strongly favor C-type inactivation, resulting in inactivation rates that are very similar in the presence or absence of the inactivation peptide. The data in Fig. 1 suggest that in both Na^+ and K^+ ionic conditions, the inactivation peptide has little influence on the overall rate of recovery from inactivation, despite the dramatic effects of the inactivation ball on the time course of inactivation.

A critically important feature of the experimental traces in Fig. 1, D and E, is the presence of inward tail currents during the recovery period, despite nearly complete inactivation of either the Kv1.4N/Kv1.5 chimera (Fig. 1 D) or WT Kv1.5 (Fig. 1 E). To clarify these events in more detail, Fig. 2 distinguishes two very different types of recovery tails that can be observed in Kv channels. Under the physiological condition of relatively low extracellular K^+, blockade by the inactivation peptide allows evacuation of K^+ from the pore, accelerating C-type inactivation, and rendering channels impermeant to K^+ (Baukrowitz and Yellen, 1995). These events are illustrated in the schematic diagram accompanying Fig. 2 A, and the sample trace illustrates that these experimental conditions preclude the observation of tail currents upon repolarization (Fig. 2 A). The current understanding of unbinding of the inactivation peptide has come from studies that minimize C-type inactivation, using high extracellular K^+ concentrations or specific pore mutations (Demo and Yellen, 1991; Ruppersberg et al., 1991). A representative trace of this type of experiment is depicted in Fig. 2 B, in which currents from an HEK 293 cell transiently transfected with Kv1.4 K533V (equivalent to T449V in *Shaker*) have been recorded in the presence of 135 mM extracellular K^+. The cell was pulsed to +60 mV for 600 ms, and repolarized to −100 mV to allow observation of tail currents. In this experiment, C-type inactivation has not occurred, and the tail currents observed during repolarization result from currents passing through channels in the open state as the inactivation peptide unbinds from the pore (see Fig. 2 B schematic). Several previous studies have demonstrated that binding of intracellular blockers, such as quaternary ammonium ions or the inactivation peptide, compete with channel closure and consequently slow tail current decay (Demo and Yellen, 1991). Thus, the rate of tail current decay in Fig. 2 B is influenced by the binding properties of the inactivation peptide to the open pore as it is closing.

In contrast, the traces shown in Fig. 1, D and E, and Fig. 2 C were collected under ionic conditions that strongly favor C-type inactivation (i.e., 135 $Na^+_{i/o}$, occasionally supplemented with very small concentrations of extracellular K^+), yet they clearly exhibit significant inward tail currents. The schematic diagram accompanying Fig. 2 C illustrates the origin of the recovery tails observed in Na^+ recording conditions. Previous studies have shown that the conformational changes of C-type inactivation result in a change in the relative permeabilities of Na^+ and K^+ ions. In the absence of K^+ ions, C-type–inactivated channels exhibit a significant conductance for Na^+ (Starkus et al., 1997; Kiss et al., 1999). Also, during recovery from inactivation, channels occupy one or more states with a large Na^+ permeability (labeled Na^+-permeable states in the diagram), allowing for the observation of significant inward Na^+ tails during recovery from inactivation (Wang et al., 2000). Thus, the recovery tails recorded in Na^+ conditions reflect channel occupancy of Na^+-permeable states during recovery from C-type inactivation. Given the effects of the inactivation peptide on the kinetics of deactiva-

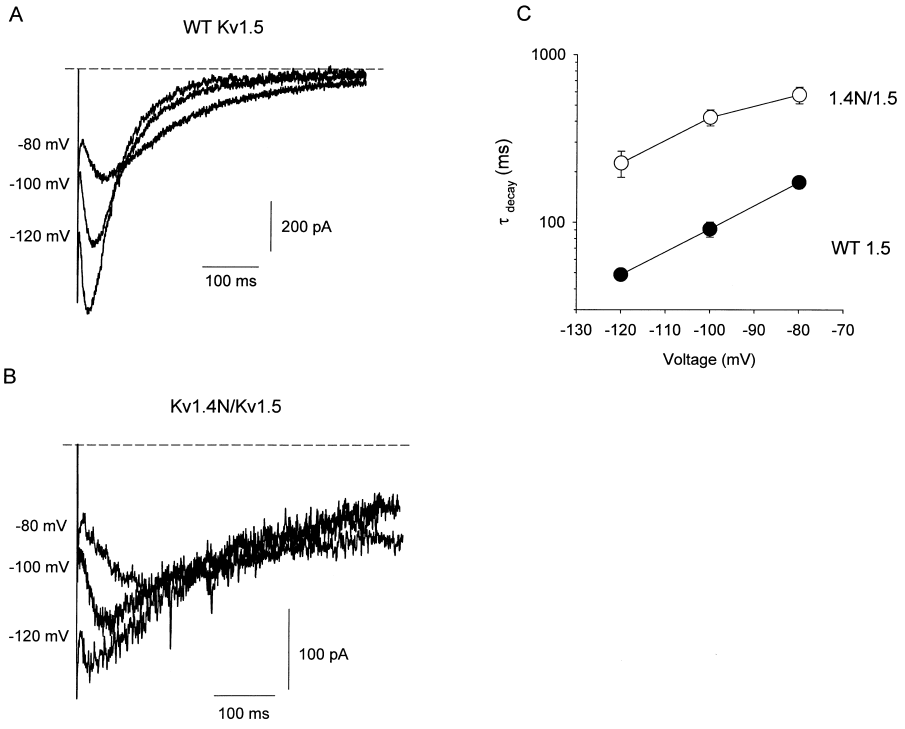

FIGURE 3. Slowing of Na^+ tail current decay by the Kv1.4 inactivation peptide. HEK 293 cells expressing (A) WT Kv1.5 or (B) Kv1.4N/Kv1.5 were depolarized to +60 mV for 800 ms and repolarized to −80, −100, or −120 mV to observe Na^+ tail currents. Representative traces in each panel were collected from the same cell, and currents were recorded in symmetrical 135 mM Na^+ conditions, with 1 mM K^+ supplemented to the extracellular solution. (C) The decay phase of the slow tails was fit with a single exponential function, and mean time constants (3–5 cells per point) have been compiled for Kv1.4N/Kv1.5 (open circles) and WT Kv1.5 channels (filled circles). Clearly, the presence of the inactivation peptide results in significant slowing of the Na^+ tail current at all recovery potentials examined.

tion of open channels, we hypothesized that interactions between the inactivation peptide and C-type–inactivated channels may influence the properties of the Na^+ recovery tail current. Despite the apparently invisible effects of the inactivation peptide on the rate of recovery from inactivation (Fig. 1 C), we have noticed several dramatic effects of the inactivation peptide on the Na^+ recovery tail. In the following sections, we compare the Na^+ recovery tail currents of WT Kv1.5 (C-type inactivation only) and the Kv1.4N/Kv1.5 chimera (C-type and N-type inactivation), and describe three major effects of the inactivation peptide on the properties of the slow Na^+ tail of C-type–inactivated channels.

Slowed Recovery Tails by the Inactivation Peptide

The representative traces in Fig. 3 A depict Na^+ tail currents recorded from WT Kv1.5 channels at recovery potentials between −80 and −120 mV, following an 800-ms depolarizing pulse to +60 mV. Na^+ tail current recordings from Kv1.5 exhibit a very prominent rising phase, followed by a slow decay taking many hundreds of milliseconds. We interpret the properties of the Na^+ tail currents using the state diagram shown in Scheme I (Wang et al., 2000). In this scheme, channels that undergo C-type inactivation recover through a highly Na^+-permeable "R" state. Entry of channels into the R state during recovery accounts for the prominent rising phase of the inward tail current, and deactivation of channels from the R state into closed-inactivated (CI) states accounts for the decay of the inward tail.

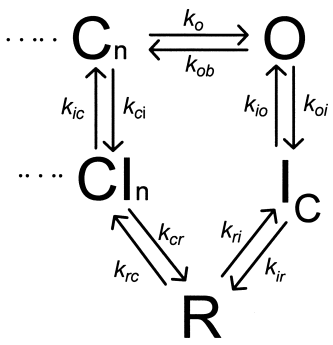

SCHEME I

The first important effect of the inactivation peptide is a significant slowing of the decay time constant of the Na^+ tail currents. This effect is illustrated by the representative traces in Fig. 3 B, which depict Na^+ tail currents recorded from the Kv1.4N/Kv1.5 chimeric channel, at recovery potentials between −80 and −120 mV. Na^+ tail current recordings from both WT Kv1.5 (Fig. 3 A) and Kv1.4N/Kv1.5 (Fig. 3 B) exhibit a very prominent rising phase. However, in the presence of the inactivation peptide, the rate of channel closure is slowed significantly. This observation is summarized in the mean data presented in Fig. 3 C. At all potentials examined, the rate of tail current decay was more than fourfold slower in the Kv1.4N/Kv1.5 chimera. This observation demonstrates an interaction between the inactivation peptide and the pore of channels that have undergone C-type inactivation, suggesting that the C-type–inactivated pore forms a patent receptor for the inactivation peptide.

Blockade of Inward Na^+ Tails by the Inactivation Peptide

A second feature of the modulation of the Na^+ tails by the inactivation peptide is a significant reduction of the inward tail current. Data in Fig. 4 A illustrates normalized representative current recordings from HEK 293 cells expressing either WT Kv1.5 or Kv1.4N/Kv1.5. Since Kv1.5 channels conduct a prominent outward current before inactivating, the magnitude of the inward tail current can be compared with the peak outward current to assess current blockade by the inactivation ball. The representative traces in Fig. 4 A have been normalized to their peak outward currents, and clearly demonstrate that the peak inward tail current is much smaller relative to the peak outward current in the Kv1.4N/Kv1.5 construct. In this experimental condition (tails at −100 mV, 135 mM $Na^+_{i/o}$ + 1 mM K^+_o), the ratio of peak tail current/peak outward current was 0.43 ± 0.04 in WT Kv1.5 (n = 6), and 0.12 ± 0.01 in Kv1.4N/Kv1.5 (n = 5) (Fig. 4 B). Thus, interaction of the channel with the inactivation peptide in Kv1.4N/Kv1.5 results in an ∼75% reduction of the magnitude of the inward recovery tail current. Also evident in Fig. 4 A is a crossover of tail currents from WT Kv1.5 and Kv1.4N/Kv1.5 channels (marked with an asterisk), providing a clear demonstration of the slowing of tail current kinetics by the inactivation peptide described in Fig. 3.

Delayed Peak of the Slow Na^+ Tail

As shown in the previously described current recordings, the inward Na^+ recovery tail exhibits a prominent rising phase, which reflects the entry of channels into highly Na^+-permeable states during recovery from inactivation. Fig. 4 C illustrates representative tail current recordings from WT Kv1.5 and Kv1.4N/Kv1.5, enlarged to show the region of peak current. These recordings show that the presence of the inactivation peptide results in a clear delay in the time to peak of the inward tail current. This superimposition of tail currents reinforces the idea that the inactivation peptide is not solely responsible for the rising phase of the Na^+ tail current. However, the presence of the inactivation peptide prolongs the slow rising phase. In this experimental condition (tails at −100 mV, 135 mM $Na^+_{i/o}$ + 1 mM K^+_o), the presence of the inactivation ball delays the time to peak current roughly twofold, in-

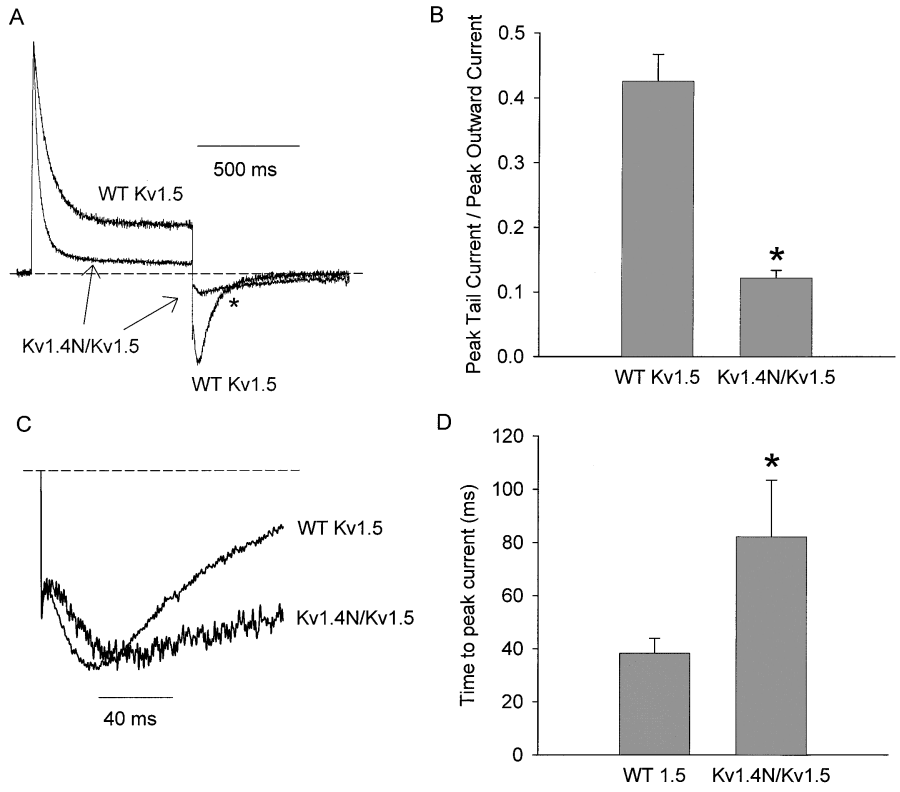

FIGURE 4. Blockade and delay of peak tail current by the Kv1.4 inactivation peptide. HEK 293 cells expressing WT Kv1.5 or Kv1.4N/Kv1.5 were depolarized to +60 mV for 500 ms and repolarized to −100 mV to observe Na^+ tail currents. Representative traces depicted in A have been normalized to their respective peak outward current, to illustrate the different magnitude of the inward tail current relative to the peak outward tail current. (B) Mean data in which the magnitude of the inward tail current has been normalized to the peak outward current in cells expressing Kv1.4N/Kv1.5 or WT Kv1.5 under identical recording conditions. This reduction of the inward tail current magnitude was observed at all recovery potentials examined (−80, −100, and −120 mV) and in the presence or absence of 1 mM extracellular K^+. Tail currents depicted in C have been normalized to the peak tail current, and expanded around the region of the peak tail current. The Kv1.4N/Kv1.5 chimeric channel consistently exhibited a prolonged delay to the peak tail current, compared with the WT Kv1.5 channel. Panel D illustrates mean data of the delay to the peak inward tail current in Kv1.4N/Kv1.5 or WT Kv1.5. Asterisks denote a statistically significant difference (Student's *t* test) with $P < 0.05$.

creasing the time to peak current from 38 ± 6 ms in WT Kv1.5 (n = 6) to 82 ± 21 ms (n = 5) in Kv1.4N/Kv1.5 (Fig. 4 D).

Common Effects in Kv1.5 and Kv1.4

The features of the slow Na^+ tail described thus far have all been characterized in the Kv1.4N/Kv1.5 chimeric channel—this permits the convenient measurement of both outward and inward currents, and allows us to normalize tail current magnitude to peak outward current. We have also observed similar effects of the Kv1.4 inactivation peptide in the native background of the Kv1.4 channel (Fig. 5 A). Cells expressing Kv1.4 in symmetrical Na^+ conditions were pulsed to +60 mV for 2 or 800 ms, and repolarized to −100 mV for tail current measurement. As mentioned previously, Kv1.4 exhibits a high sensitivity to extracellular K^+ concentrations (Pardo et al., 1992), so the slow Na^+ tail currents characteristic of C-type–inactivated channels appear after even very brief depolarizations (Fig. 5 A, 2 ms pulse). The tail current kinetics observed after brief depolarizations in Kv1.4 are indistinguishable from the tail currents observed in NH_2-terminally deleted forms of Kv1.4 (unpublished data). Longer depolarizations (Fig. 5 A, 800-ms pulse) allow time for the inactivation peptide to bind to the channel, and result in Na^+ tail currents qualitatively similar to those observed in the Kv1.4N/Kv1.5 chimera (compare Fig. 5, A and B). After the onset of inactivation ball binding, the Kv1.4 Na^+ tail currents exhibited a slowed rising phase resulting in a delayed peak tail current, and a slower rate of tail current decay. We found it difficult to quantify the blockade of the inward tail current by the inactivation ball as was done for Kv1.5 (Fig. 4), because Kv1.4 did not conduct any outward currents to allow normalization of traces.

We also emphasize an important difference between the tail currents recorded from Kv1.5 (Fig. 5 B) and Kv1.4 (Fig. 5 A): inactivation ball binding occurs in different channel states in these two constructs. Kv1.5 readily conducts outward Na^+ current through the open state upon depolarization, and thus is subjected to N-type inactivation from the open state. In contrast, Kv1.4 conducts minimal outward Na^+ current upon depolarization, because this channel is very sensitive to reductions in extracellular K^+ concentration. Since slow Na^+ tails are apparent after even very brief depolarization of Kv1.4, it is likely that in 0 K^+ conditions Kv1.4 is either permanently C-type inactivated, or undergoes

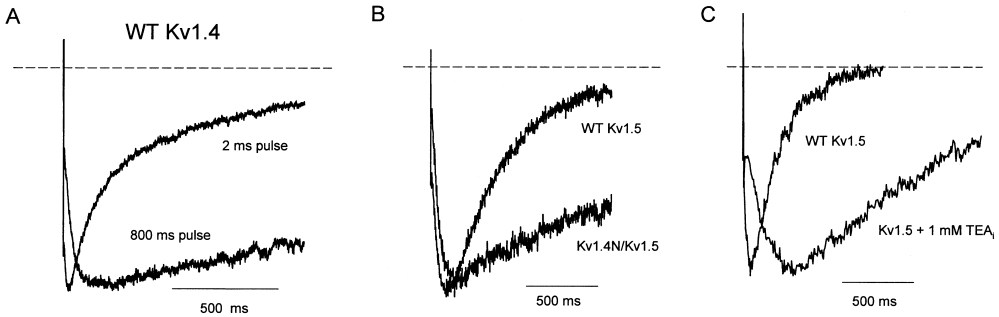

FIGURE 5. Common effects of the inactivation peptide and quaternary ammonium ions in Kv1.4 and Kv1.5. (A) Cells expressing WT Kv1.4 were pulsed to +60 mV for either 2 or 800 ms and repolarized to −100 mV to observe tail currents. Tail currents have been expanded and normalized to the peak current. Slowing of tail current decay is apparent with longer depolarizations that allow binding of the inactivation peptide. (B) Currents were recorded from cells expressing either WT Kv1.5 or Kv1.4N/Kv1.5 in 135 mM $Na^+_{i/o}$. Cells were depolarized to +60 mV for 400 ms, followed by a repolarization to −100 mV. Tail currents have been expanded and normalized to the peak current to illustrate the time course of decay in the presence and absence of the inactivation ball. (C) Na^+ tail currents recorded from WT Kv1.5 in the presence or absence of 1 mM TEA_i have been normalized to peak current to observe the slowing of tail current resulting from interactions of the C-type–inactivated channel with intracellular quaternary ammonium ions.

C-type inactivation almost instantaneously upon depolarization. Similar Na^+ currents are seen in Kv1.5 when recordings are made at low pH, a condition that dramatically accelerates Kv1.5 inactivation (Zhang et al., 2003). Also, the K^+ sensitivity of Kv1.4 is abolished by the K533V mutation (equivalent to *Shaker* T449V), which has been implicated in C-type inactivation in many prior studies. Therefore, in Na^+ recording conditions, the inactivation ball likely binds primarily to the C-type–inactivated state of Kv1.4. Despite inactivation peptide binding occurring in different channel states, the effects of the inactivation peptide are similar between Kv1.5 and Kv1.4, suggesting that the inactivation peptide binds to both the open and C-type–inactivated channel states. Furthermore, Kv1.4 channels must be held at a depolarized potential to observe an effect of the inactivation peptide. This confirms that even in C-type–inactivated channels, access of the inactivation peptide to its binding site is gated, and that depolarizing potentials can open the activation gate of inactivated channels.

Inclusion of quaternary ammonium ions in the pipette filling solution mimics the slowing of the Na^+ tail current decay caused by the inactivation peptide (Fig. 5 C). The representative traces depict tail currents recorded from HEK 293 cells expressing WT Kv1.5 channels, in the presence and absence of 1 mM intracellular TEA. In the presence of intracellular TEA, the inward Na^+ tails are slowed considerably, and the time to peak current is significantly delayed. Similar findings were observed with other quaternary ammonium blockers in both WT Kv1.5 and WT Kv1.4 channels (10 μM tetrabutylammonium, 10 μM tetrapentylammonium; unpublished data). These data clearly illustrate an interaction between the inactivation peptide, or quaternary ammonium ions, and the pore of channels that have undergone C-type inactivation.

As mentioned previously, by using Na^+ recording conditions in our experimental approach, we are able to observe the properties of inactivation peptide unbinding from both the open and C-type–inactivated channel states in identical ionic conditions. With an understanding of the effects of the inactivation peptide on the slow Na^+ tail, we generated two further objectives. First, we have used C-type inactivation–removed channel mutants to contrast inactivation peptide binding to the open and C-type–inactivated states. Second, we have used kinetic modeling and computer simulations to evaluate possible mechanisms underlying our observations, to explore the events involved in recovery from N- and C-type inactivation.

C-type Inactivation–deficient Channels Exhibit Incomplete N-type Inactivation

Previous studies have suggested that recovery from C-type inactivation remains limiting in Kv1.4 even in conditions (e.g., high extracellular K^+) designed to minimize the onset of C-type inactivation (Rasmusson et al., 1995). To ensure separation of the effects of C-type inactivation from those of N-type inactivation, we have used mutations in Kv1.4 (K533V) and Kv1.5 (R487V) that are equivalent to the T449V mutation in *Shaker*, and have been shown to significantly reduce C-type inactivation (Lopez-Barneo et al., 1993). We have observed empirically that the slowing of inactivation by these mutations is very dramatic when recordings are performed in symmetrical Na^+ conditions (in the absence of any permeating K^+) (Wang et al., 2000). Confirming this result in Kv1.4, data in Fig. 6 illustrates the absence of inactivation in the Kv1.4 K533V mutant with Na^+ as the permeant ion. Unlike ball-deleted WT Kv1.4 or Kv1.4 K533V in K^+ conditions, the Na^+ condition dramatically reduces the extent of slow inactivation (Fig. 6). Thus, we are confident that the Kv1.5 R487V

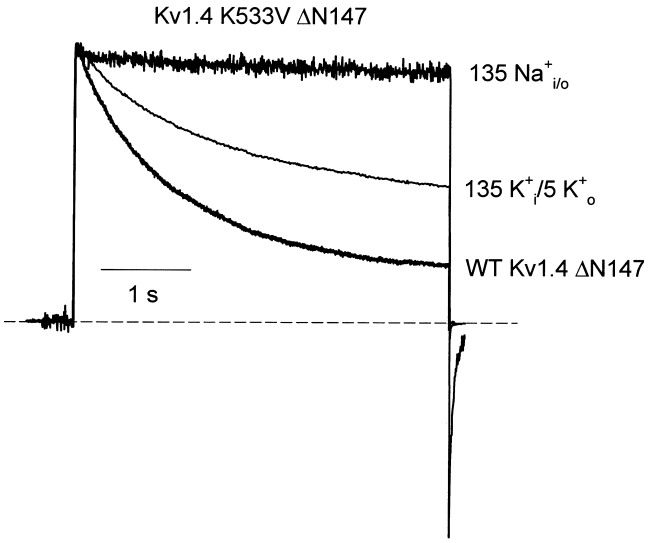

FIGURE 6. A Kv1.4 C-type inactivation–deficient channel mutant. C-type inactivation was removed from Kv1.4 with the K533V mutation. HEK 293 cells expressing Kv1.4 K533V ΔN147 were depolarized for 4 s at +60 mV, from a holding potential of −100 mV, in the ionic conditions described in the Figure. In $135K^+_i/5K^+_o$, the K533V mutation attenuates the decay of outward current. In 135 $Na^+_{i/o}$, the K533V mutation essentially abolishes any decay of outward current. Representative currents exhibiting C-type inactivation in WT Kv1.4ΔN147 are also shown for reference.

or Kv1.4 K533V mutations provide an effective means of reducing C-type inactivation, whether Na^+ or K^+ is the permeating ion. Very importantly, even with prolonged depolarizations in symmetrical Na^+ conditions, the Kv1.5 R487V or Kv1.4 K533V channels never develop the slowly decaying Na^+ tails associated with the onset of C-type inactivation (Starkus et al., 1997; Wang et al., 2000). This feature of the tail currents provides a valuable experimental index of the state of the pore—the absence of a slow Na^+ tail current confirms that channels have not undergone C-type inactivation. We have used these C-type inactivation–deficient systems to examine the influence of the inactivation peptide on the open pore, in ionic conditions identical to those used to characterize ball binding to C-type–inactivated channels.

When the full-length Kv1.4 K533V channel, with an intact NH_2-terminal inactivation peptide, was depolarized in symmetrical Na^+ (Fig. 7 A), a rapidly decaying current was observed, confirming the persistence of N-type inactivation. However, we made the surprising observation that the N-type inactivation process left a much larger steady-state current than in channels with an intact C-type inactivation mechanism (compare Figs. 7 A and 1, A and D). C-type inactivation–deficient channels appeared to inactivate by only 71 ± 2% (n = 6), compared with the >95% inactivation routinely observed in WT channels (Fig. 1 A). This effect was slightly more pronounced in a chimeric channel consisting of the NH_2 terminus of Kv1.4 fused to the Kv1.5 R487V channel, which exhibited only 63 ± 2% (n = 6) inactivation in this experiment (Fig. 7 B).

The Kv1.4 K533V or Kv1.5 R487V mutations did not markedly affect the rate of current decay due to N-type inactivation in Na^+ conditions. This observation is consistent with previous reports, which have demonstrated insignificant effects of these and similar mutations on the rate of N-type inactivation by the Kv1.4 inactivation peptide (Baukrowitz and Yellen, 1995; Rasmusson et al., 1995). However, others have not reported the weaker steady-state block that we have observed, suggesting that it may be a unique feature of Na^+ permeation (Fig. 7, A and B). One intriguing explanation is that the R487V or K533V mutations do not completely abolish C-type inactivation in K^+ conditions, and that a residual inactivation process contributes to the enhanced steady-state block seen in K^+ conditions. Fig. 6 clearly demonstrates that the Kv1.4 K533V mutant inactivates markedly more slowly in Na^+ conditions compared with K^+ conditions, and similar results are observed in Kv1.5 (Wang et al., 2000). In addition, the R487V mutation of Kv1.5 and even the T449V mutant of *Shaker* both exhibit considerable slow inactivation in K^+ conditions, and this inactivation process is essentially abolished when Na^+ is substituted for K^+ (Fig. 6) (Wang et al., 2000; Starkus et al., 2003). A second possible explanation for this observation is an ion dependence of the affinity between the inactivation peptide and the channel, possibly arising from slight conformational changes of the open state when Na^+ is the primary permeant ion. Importantly, since the Kv1.4 K533V (compare Fig. 2, A and B) or Kv1.4 K533Y mutations (Rasmusson et al., 1995) have no significant effect on the inactivation peptide affinity in K^+ recording conditions, it seems likely that our observation of weaker steady-state block is due to the altered ionic conditions, and not the outer pore mutation. However, we cannot exclude the possibility of a unique interaction between the Na^+ recording conditions and the K533V mutation.

N-type inactivation in the C-type inactivation–deficient channels also resulted in significant slowing of the deactivation tails. In the Kv1.4 K533V channel, the time constant of deactivation was 42.1 ± 6.7 ms after a brief depolarization (10 ms in Fig. 7 A), but was slowed to 65.5 ± 6.1 ms after the onset of N-type inactivation. Similarly in the Kv1.4N/Kv1.5 R487V chimeric channel, time constants of deactivation were measured as 8.4 ± 0.8 ms after a brief depolarization and 28.7 ± 1.7 ms after the onset of N-type inactivation (Fig. 7 B). This slowing of deactivation is consistent with unbinding of the inactivation peptide limiting the rate of channel closure (Demo and Yellen, 1991). Furthermore, the deactivation tail currents after N-type inactivation exhibit

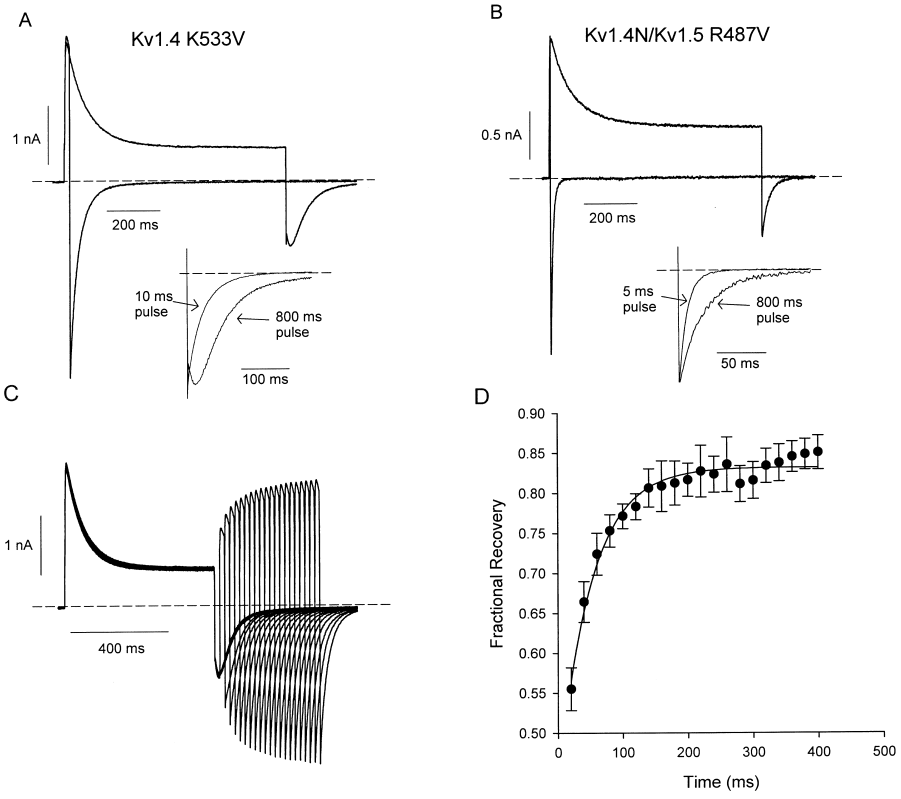

FIGURE 7. N-type inactivation in C-type inactivation–deficient Kv channels. Currents were recorded from cells expressing (A) Kv1.4 K533V or (B) a chimeric construct of Kv1.5 R487V and the NH_2 terminus of Kv1.4, in symmetrical Na^+ recording conditions. Cells were depolarized to +60 mV from a holding potential of −100 mV for a brief pulse (5–10 ms) or 800 ms, and repolarized to −100 mV. Current tracings from the short and long protocols are overlaid in each panel. The insets in A and B depict normalized tail currents after the brief and long depolarizing pulses, illustrating the slowing of tail currents after binding of the inactivation peptide. (C) Recovery from N-type inactivation in a C-type–deficient channel (Kv1.4 K533V) was measured with a double pulse protocol, consisting of a 600-ms depolarizing prepulse to +60 mV, followed by a variable recovery period at −100 mV and a brief test pulse to +60 mV. Experiments were conducted in symmetrical Na^+ recording conditions. (D) The envelope of peak test pulse currents in C was fit with a single exponential equation yielding a mean time constant of 53.5 ± 5.5 ms (n = 4). Tail current decay in this experiment had a mean time constant of 62.3 ± 3.1 ms (n = 4).

mild biphasic kinetics, with a very brief rising phase preceding tail current decay (Fig. 7 A, inset, and C). This feature is consistent with the "hooked tails" observed previously during *Shaker* deactivation in high K^+ conditions (Demo and Yellen, 1991). Tail currents recorded from the Kv1.4N/Kv1.5 R487V chimeric channel exhibited no significant biphasic kinetics, but were clearly slowed by the onset of N-type inactivation (Fig. 7 B, inset).

In the K533V mutant channel, C-type inactivation appears to be essentially eliminated in the symmetrical Na^+ condition (Fig. 6). Consequently, the rate of recovery from N-type inactivation in this condition should be very similar to the rate of tail current relaxation, as both should be limited by the rate of peptide ball unbinding. We have examined this relationship in the double-pulse experiment in Fig. 7 C, in which cells expressing Kv1.4 K533V channels were depolarized to +60 mV for 600 ms followed by a variable recovery period and a test pulse to +60 mV to observe the extent of recovery from inactivation (ball unbinding). In four cells tested, we confirmed this idea by showing that peak current recovery of Kv1.4 K533V occurred with a time constant of 53.5 ± 5.5 ms (Fig. 7 D), while tail current recovery after N-type inactivation occurred with a time constant of 62.3 ± 3.1 ms. It is noteworthy that we also consistently observed a slow component to recovery in these channels, although we are unsure of the mechanism underlying this process. We have included only a fit of the rapid component of recovery here, because this represents the largest component of recovery, and mirrors the kinetics of tail current decay in both Kv1.5 K533V and Kv1.4N/Kv1.5 R487V. This analysis of the Kv1.4 K533V and Kv1.5 R487V channels provides a benchmark with which to compare the effects of the inactivation peptide on the slow Na^+ tail currents of Kv1.4 and Kv1.5.

Summary and Model of the Slow Na^+ Tail

The data presented thus far illustrates three major effects of the Kv1.4 inactivation peptide on the slow Na^+ tails of Kv1.4 or Kv1.5: a dramatic slowing of tail current decay, a blockade of the peak inward tail current, and a slowing of the rising phase of the Na^+ tail current. The experiments presented thus far clearly suggest an interaction between the inactivation peptide and the C-type–inactivated pore, and qualitatively resemble the effects of the inactivation peptide on channel deactivation from the open state. We have used our characterization of inactivation ball binding to the open and C-type–inactivated channel states to construct and evaluate kinetic models and

to investigate the steps involved in recovery from inactivation.

Our final kinetic model is based on previously published versions describing the pathway of recovery from inactivation of Kv1.5, shown in Scheme I. We have considered several other hypotheses regarding inactivation peptide binding after C-type inactivation. However, for brevity, we present a simple model in Fig. 8 A that duplicates our experimental results, and illustrates the most important conclusion of our modeling, which is that binding of the inactivation peptide to the C-type state is required to explain the effects of the inactivation peptide on the C-type–inactivated Na^+ tail current (for additional modeling considerations, see online supplemental material, available at http://www.jgp.org/cgi/content/full/jgp.200308956/DC1). In Fig. 8 A, we have simply added two additional states to Scheme I: an N-type–inactivated state (I_N), and a state that has undergone both C- and N-type inactivation ($I_{N,C}$). The state diagram in Fig. 8 A explains the slowed tail current decay (Fig. 3 B and C) and the delayed time to peak current (Fig. 4, C and D) as follows. Stable inactivation ball binding to the I_C state results in slow exit of channels from the $I_{N,C}$ state to the I_C state and consequently slower transit of channels through the highly Na^+-permeable R state. This slower transit of channels through the R state also accounts for the observed apparent blockade of inward current (Fig. 4, A and B), because there is a lower occupancy of the R state throughout recovery.

We have used this kinetic scheme to generate the simulations presented in Fig. 8 B, which duplicate the experimental features of the slow Na^+ tail current characterized in Figs. 3–5. Currents depicted by the solid trace represent simulations of WT Kv1.5, in the absence of N-type inactivation, whereas currents depicted by the dashed traces represent simulations of the Kv1.4N/Kv1.5 chimera (N- and C-type inactivation). These data demonstrate the apparent blockade resulting from slow unbinding of the inactivation ball from the C-type–inactivated state, and also exhibit the tail current crossover observed in Fig. 4 A. Tail currents from both simulations have been expanded and normalized in the inset to Fig. 8 B, showing that the model also duplicates the considerable slowing of tail current decay resulting from interactions between N- and C-type inactivation (compare with Fig. 3 and Fig. 5), and the prolonged

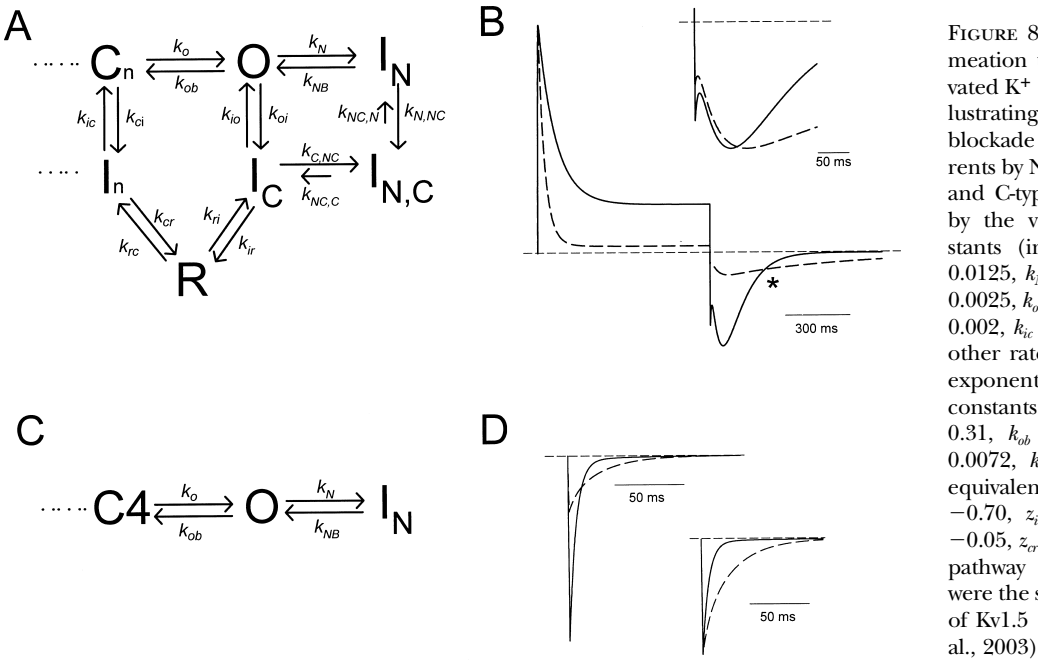

FIGURE 8. Kinetic model of Na^+ permeation through N- and C-type–inactivated K^+ channels. (A) State diagram illustrating a mechanism for the apparent blockade and slowing of Na^+ tail currents by N-type inactivation. Rates for N- and C-type inactivation were governed by the voltage-independent rate constants (in ms^{-1}) $k_N = 0.025$, $k_{NB} = 0.0125$, $k_{N,NC} = 0.1$, $k_{NC,N} = 0.006$, $k_{io} = 0.0025$, $k_{oi} = 0.01$, $k_{C,NC} = 0.0167$, $k_{NC,C} = 0.002$, $k_{ic} = 0.000055$, $k_{ci} = 0.00008$. All other rates depicted were governed by exponential functions of voltage. Rate constants at 0 mV were (in ms^{-1}) $k_o = 0.31$, $k_{ob} = 0.011$, $k_{ir} = 0.001$, $k_{ri} = 0.0072$, $k_{rc} = 0.017$, $k_{cr} = 0.185$, and equivalent valences were $z_o = 0.60$, $z_{ob} = -0.70$, $z_{ir} = -0.65$, $z_{ri} = 0.55$, $z_{rc} = -0.05$, $z_{cr} = 0.05$. Rates in the activation pathway (not shown in this diagram) were the same as in our previous models of Kv1.5 (Kurata et al., 2001; Zhang et al., 2003). (B) Simulations of WT Kv1.5 (solid trace) and Kv1.4N/Kv1.5 (dashed trace) currents recorded in 135 mM $Na^+_{i/o}$ + 1 mM K^+_o. Currents were simulated during a 800-ms depolarization to +60 mV, followed by a 800-ms repolarization to −100 mV, reproducing the experiment depicted in Fig. 4 A. To simulate Kv1.4N/Kv1.5, all the rates described in panel A were used. To simulate Kv1.5, transitions to and from N-type–inactivated states (k_N, k_{NB}, $k_{C,NC}$, $k_{NC,C}$) were removed from the model. (Inset) The tail currents in B have been expanded and normalized to peak current, to illustrate the prolonged delay and slower decay of the Na^+ tail in the presence of the inactivation peptide. (C) All transitions to and from the C-type–inactivated states have been removed from the state diagram in A to simulate currents through C-type inactivation–deficient channels (e.g., R487V). (D) Tail currents at −100 mV simulated using the state diagram in C. Solid traces were simulated with an initial condition of 100% of channels in the open state, while the dashed traces were simulated with an initial condition of 30% of channels open, and 70% of channels in the N-type–inactivated state. Rate constants were (in ms^{-1}) $k_N = 0.025$, $k_{NB} = 0.05$, $k_o = 0.31$, and $k_{ob} = 0.011$, with associated valences of $z_o = 0.60$, and $z_{ob} = -0.70$. (Inset) The tail currents in D have been normalized to peak current to illustrate slowing of tail currents after the onset of N-type inactivation.

time to peak of the Na^+ tail current (compare with Fig. 4 C).

Many of the rate constants describing ball binding/unbinding are constrained by experimental data. The rates k_N and k_{NB} were determined based on the inactivation and recovery kinetics of ball binding in C-type inactivation deficient channels (Fig. 7 A and D). The rates k_{io} and k_{oi} were determined based on the rates of C-type inactivation in WT Kv1.5 (Fig. 1 E). We also observed that the onset of the slowing of the inward Na^+ tail was slow ($\tau \sim$100 ms) in Kv1.4 (which undergoes C-type inactivation extremely rapidly in the absence of K^+), suggesting that binding of the inactivation ball to the C-type–inactivated state is slower than binding to the open state (unpublished data). This observation allowed us to roughly estimate the rate $k_{C,NC}$, which describes the rate of ball binding to the C-type–inactivated channel. However, it should be noted that the absolute value of the $k_{C,NC}$ rate has little bearing on the altered kinetics or apparent blockade of Na^+ tails by the inactivation peptide. Rather, the ratio of the rates $k_{C,NC}$ and $k_{NC,C}$ determines the extent of blockade and tail slowing (all rate constants and valencies used for simulations are summarized in the legend to Fig. 8).

Simulation of Tail Currents in C-type–deficient Channels

Simulation of currents in the absence of C-type inactivation (e.g., K533V or R487V) is more straightforward. In Fig. 8 C, we present a state diagram in which the transitions to the C-type–inactivated state have been removed. Given the absence of any current decay in Na^+ currents through R487V or K533V (ball-deleted) channels, we feel this is an accurate description of the gating of the C-type–deficient channels. In this model, binding of the inactivation peptide competes with closure of the activation gate, and therefore slows deactivation tail currents. Fig. 8 D illustrates tail current decay simulated at −100 mV in two different initial conditions. The solid trace represents the time course of tail current decay with an initial condition of all channels occupying the open state, to approximate the short pulses in Fig. 7, A and B. The dashed traces represent the time course of tail current decay with an initial condition of 30% of channels occupying the open state, and 70% occupying the N-type–inactivated state, to approximate the 800 ms pulses in Fig. 7, A and B. Clearly, the onset of N-type inactivation results in much slower tail current decay.

To reasonably simulate the extent of tail current slowing observed experimentally in the Kv1.4N/Kv1.5 R487V chimera (Fig. 7 B), this model required acceleration of the unbinding rate of the inactivation peptide (k_{NB}) compared with the value required to accurately simulate outward currents. This likely arises from an effective voltage-dependence of ball unbinding, caused by a "knock-off" effect of inward ionic currents, and previously described by Demo and Yellen (1991), among others. To reproduce the extent of N-type inactivation of outward currents (Fig. 8 B), the rate of inactivation peptide unbinding (k_{NB}) was set to be 50% of the binding rate (k_N). However, to accurately simulate the tail current decay in Fig. 8 D, the unbinding rate (k_{NB}) was set to be double the binding rate (k_N). In contrast, our simulation of the Na^+ tail currents through channels with intact N- and C-type inactivation (e.g., Kv1.4N/Kv1.5) were most representative of the data with an unbinding rate from the C-type–inactivated state ($k_{NC,C}$, Fig. 8 A) of five- to eightfold smaller than the binding rate ($k_{C,NC}$) to reasonably simulate the slowing of the C-type–inactivated Na^+ recovery tail current.

The surprising implication of these rate constants is that the onset of C-type inactivation increases the affinity between the pore and the inactivation peptide. Although quantitative estimates of affinity are not possible (because the effective concentration of the inactivation peptide at the intracellular mouth of the pore is unknown), the ratios of the binding and unbinding rate constants give an estimate of the relative change in affinity. Based on the rate constants just discussed (Fig. 8, legend), our modeling suggests that C-type inactivation enhances the affinity between the inactivation peptide and the pore by at least 10-fold.

DISCUSSION

In the current study, we have examined inactivation ball binding to the open state and C-type–inactivated state by exploiting the properties of Na^+ permeation through K^+ channels, particularly the ability of inactivated K^+ channels to conduct Na^+ currents. This experimental approach offers insight into the structural changes associated with C-type inactivation and recovery, and contrasts the different binding properties of the inactivation peptide to the open state and the C-type–inactivated state of the channel.

Mechanism of Slowing of the Na^+ Tail by the Inactivation Peptide

We observed that the Kv1.4 inactivation peptide and quaternary ammonium ions exert effects on the C-type–inactivated Na^+ tail currents which resemble the effects of these agents on the deactivating tail currents of open channels. That is, these agents were shown to reduce the peak tail current, delay the peak tail current (intracellular blockers often impart "hooked" deactivation tail currents), and slow the decay of the C-type–inactivated Na^+ tail. We stress, however, that the mechanism underlying the effects on the C-type–inactivated Na^+ tail currents is subtly different. The effects on the slow Na^+ tail current result from the binding of inactivation

peptides or quaternary ammonium ions to the C-type–inactivated channel pore. This stable binding delays the appearance of the highly Na^+-permeable states normally visited during recovery from inactivation, and slow transit of channels through the Na^+-permeable R state results in an apparent blockade and slow decay of the inward tail current (Wang et al., 2000). We have evaluated other possible kinetic schemes describing the interaction of the inactivation peptide with C-type–inactivated channels (see online supplemental material, available at http://www.jgp.org/cgi/content/full/jgp.200308956/DC1), and we have found that a direct interaction of the inactivation peptide or quaternary ammonium ions with the C-type–inactivated channel pore is required to explain the kinetic effects on the tail current. Models that exclude peptide binding from the C-type–inactivated state, and only permit binding to recovery states, fail to duplicate the delayed peak tail current consistently observed in our experiments.

Inactivation Ball Binding to the C-type–inactivated State—Structural Considerations

The first important insight provided by our experiments relates to binding of the inactivation ball to the C-type–inactivated state of the channel. It is known that inhibition of C-type inactivation by high extracellular K^+ conditions results in the observation of "recovery tails" (reopening of channels during recovery from N-type inactivation) in both *Shaker* and Kv1.4 channels (Demo and Yellen, 1991; Ruppersberg et al., 1991). In these conditions, the presence of the inactivation peptide results in a reduction of inward tail currents, and slower tail current decay. All of these features are explained by the "ball and chain" model of N-type inactivation, in which the inactivation peptide is thought to bind the large inner vestibule of the K^+ channel pore (Zhou et al., 2001). Our experiments clearly demonstrate marked effects of the inactivation peptide on the Na^+ tail currents in both Kv1.5 and Kv1.4.

There is some uncertainty in the literature regarding the conformational changes underlying C-type inactivation. There is considerable evidence for conformational changes in the selectivity filter and the outer pore mouth during C-type inactivation (Liu et al., 1996; Loots and Isacoff, 1998). However, little is known about the conformation of the inner pore mouth, and recent structural advances have not addressed the process of C-type inactivation. Based on changes in the Kv1.4 C-type inactivation properties in response to altered intracellular tonicity, one recent study has suggested that the inner pore mouth undergoes a significant reduction in volume during C-type inactivation, similar in magnitude to the volume change associated with deactivation (Jiang et al., 2003a). This structural description of C-type inactivation is difficult to resolve with our data, for several reasons. In particular, our experiments demonstrate that the inactivation peptide, and quaternary ammonium ions, can exert similar effects on the Na^+ tail current whether they bind to open (Kv1.5) or C-type–inactivated (Kv1.4) channels (Fig. 5). These experiments suggest that the binding site(s) for quaternary ammonium ions and the inactivation peptide are accessible in both open and C-type–inactivated channels. Given the strong structural (Zhou et al., 2001) and biophysical/mutagenic (Choi et al., 1991, 1993) evidence that the quaternary ammonium binding site lies deep in the inner vestibule near the selectivity filter, these results suggest that the activation gates are open and the inner pore is accessible to the cytosol before, and after, C-type inactivation. Furthermore, in *Shaker* and other Kv1 channels, channel closure does not occur if a quaternary ammonium ion is in the pore. TEA, TBA, and other quaternary ammonium ions are very poorly "trapped" by Kv1 channels, and actually compete with channel closure. Thus, if C-type inactivation involves a conformational change of the inner vestibule similar to channel closure, one would expect intracellular quaternary ammonium ions to antagonize C-type inactivation, much like they antagonize deactivation. The opposite is clearly true, with quaternary ammonium ions promoting C-type inactivation of Kv1 channels (Baukrowitz and Yellen, 1996).

Importantly, the clear ability of the inactivation peptide to interact with C-type–inactivated Kv1.4 channels remains dependent on both time and membrane depolarization (Fig. 5 A). This suggests that the activation gates of inactivated channels are able to open in response to depolarization and that the inner vestibule remains exposed in the C-type–inactivated conformation. Nevertheless, conformational changes at the inner pore are likely to occur during C-type inactivation. Our data suggests the possibility of enhanced channel affinity for the inactivation peptide following C-type inactivation, which may be indicative of a conformational change in the inner vestibule (see below). As pointed out by Jiang et al. (2003a), C-type inactivation of Kv channels appears to exclude binding of certain open state blockers such as 4-AP (Castle et al., 1994). In addition, strong depolarization appears to antagonize HERG blockade by several pore blockers, suggesting competition between C-type inactivation and drug binding (Wang et al., 1997a,b). However, other evidence indicates that an intact C-type inactivation mechanism is required for potent drug block of HERG channels (Ficker et al., 1998). Our data suggests that very bulky agents including the inactivation peptide, and large quaternary ammonium ions (we have tried QA compounds as large as tetrabutylammonium and tetrapentylammonium) are able to bind and influence the

C-type–inactivated pore, indicating that a significant constriction of the inner pore (e.g., a volume change similar to deactivation) during C-type inactivation is unlikely.

Inactivation Ball Binding to the C-type–inactivated State: Gating Considerations

Although the demonstration of ball binding to C-type–inactivated channels may not be entirely surprising, to our knowledge it has not yet been demonstrated experimentally because techniques and understanding allowing for the measurement of current through inactivated channels have only recently been developed (Starkus et al., 1997, 1998; Wang et al., 2000). The obvious consequence of this finding is that reopening of K^+ channels is not obligatory during recovery from N-type inactivation. Demo and Yellen (1991) demonstrated that as the extracellular K^+ concentration is reduced, N-type inactivation results in a stronger bias toward C-type inactivation of Kv channels, so channel reopenings upon repolarization become very infrequent and recovery from inactivation is very slow. Our data and modeling are consistent with the hypothesis that the pore of channels that are both C- and N-type inactivated recover via the same pathway (albeit more slowly) as channels that are only C-type inactivated. This mechanism underlies the "silent pathway" of recovery previously described for channels that have undergone both N-type and C-type inactivation (Demo and Yellen, 1991).

A second interesting issue is that despite the significant effects of the inactivation peptides and quaternary ammonium ions on the kinetics of the C-type–inactivated Na^+ tail currents (Figs. 3–5), the effects on the rate of recovery from inactivation are clearly quite innocuous (Fig. 1, C and F). The most simple explanation for this is that even in the presence of the inactivation peptide, the time course of the Na^+ tail current is quite brief (τ on the order of hundreds of milliseconds, Fig. 3 C) compared with the overall time course of recovery from inactivation, which can take 15 s or longer to approach completion (Fig. 1 C). In addition, the kinetics of the C-type–inactivated Na^+ tail are strongly voltage dependent (Fig. 3 A, see also Fig. 7 in Wang et al., 2000), whereas the kinetics of recovery from C-type inactivation exhibit a milder voltage dependence over a similar voltage range (Kurata et al., 2001). These observations suggest one or more rate-limiting steps during recovery from C-type inactivation that govern the overall rate of recovery and minimize the effects of inactivation peptides or voltage observed in our experiments. In our previously published model of Kv1.5, for instance, recovery from C-type inactivation was governed by voltage-independent transitions between "closed-inactivated" states and "closed" states in the activation pathway (I_n and C_n in Fig. 8 A, respectively) (Kurata et al., 2001).

It should be noted that inactivation peptides are not always without influence on recovery from inactivation. Recent characterization of multiple "tandem" inactivation domains in Kv1.4 has shown that after deletion of the first inactivation domain, a second inactivation peptide (alanine-rich region comprising amino acids 39–50) can impart N-type inactivation indistinguishable from the WT channel, but slows recovery from inactivation dramatically ($\tau \sim$300 s) (Wissmann et al., 2003). Thus, in this mutant channel, it is likely that the inactivation peptide dissociates from the pore extremely slowly, and this dissociation becomes the limiting step in recovery from inactivation.

Another possible explanation arises from the prior observation that gating processes in the channel pore are not necessarily rigidly coupled to gating processes elsewhere in the channel, especially after the onset of C-type inactivation (Wang and Fedida, 2002). We have previously reported that during recovery from C-type inactivation in Kv1.5, complete recovery of gating charge occurs long before closure of the activation gate, suggesting that the channel pore can become functionally dissociated from the voltage sensors (Wang and Fedida, 2002). Thus, a second possible explanation for the very minor effects of the inactivation peptide on recovery from inactivation is that there are several independent processes occurring simultaneously during recovery. Incidentally, this phenomenon may also be reflected in the recently published crystal structure of KvAP, in which the inner pore resembles the dimensions of the open MthK structure, but the voltage paddles appear to be in a "closed" or resting configuration (Jiang et al., 2003b).

Kinetic Effects of Binding of the Inactivation Peptide

Since K^+ channels become highly permeable to Na^+ during recovery from inactivation, our experiments performed in the absence of K^+ provide some insight into the kinetics of inactivation ball binding/unbinding with C-type–inactivated channels. Surprisingly, our kinetic modeling clearly required a greater affinity of the inactivation peptide for the C-type state than the open state in order to reasonably reproduce the kinetics of the C-type–inactivated Na^+ tail (Fig. 8). This interpretation arises from our fitting of the simulated Na^+ tail currents to experimental data, but is also consistent with the requirement to maintain microscopic reversibility in the model (Fig. 8 A). That is, if binding of the inactivation peptide to the open state is considered to promote C-type inactivation, microscopic reversibility requires that the C-type–inactivated state have a greater affinity than the open state for the inactivation peptide. Also, simply by fitting the kinetics of tail

currents observed upon repolarization, we found that our model required considerably slower unbinding of the inactivation peptide from the C-type–inactivated state relative to the open state, and this translated to an estimated 10-fold or greater increase in affinity for the inactivation peptide. As discussed below, this is a surprising and intriguing finding with many implications regarding the intracellular conformation of C-type–inactivated channels. However, we stress that it remains based on a model that is, in all likelihood, imperfect. We are currently exploring a number of experimental approaches to confirm this finding independently.

Perhaps the most important implication of this finding relates to the mechanism underlying promotion of C-type inactivation after blockade by the inactivation peptide or intracellular quaternary ammonium ions. Multiple mechanisms of coupling between N- and C-type inactivation have been proposed (Rasmusson et al., 1998). These include a demonstration of the link between permeation and C-type inactivation, in which blockade of ion permeation allows for the evacuation of K^+ ions from the selectivity filter and accelerates C-type inactivation (Baukrowitz and Yellen, 1996). However, they and others have recognized that if blockade of K^+ permeation is the mechanism of coupling of intracellular blockers to C-type inactivation, then other open channel blockers should also promote C-type inactivation (simply as a consequence of their blockade of K^+ flux). This is clearly not the case for all open-channel blockers, since 4-AP appears to antagonize C-type inactivation despite its blockade of K^+ flux (Castle et al., 1994). Others have described an apparent allosteric coupling of N-type and C-type inactivation in a complex of Kvβ1.2 with Kv1.4, and more recent studies have also suggested allosteric promotion of Kv1.4 C-type inactivation by quinidine blockade or by the inactivation peptide (Morales et al., 1996). These findings have led to an "allosteric" model in which intracellular blockers bind the inner vestibule of the pore and "orient" the channel to favor C-type inactivation. Our results raise the possibility that C-type inactivation can result in an energetically more stable complex between the inner vestibule and the inactivation peptide. This stabilized interaction between the inactivation peptide and the C-type–inactivated pore may underlie, at least in part, the acceleration of C-type inactivation after binding of the inactivation peptide.

Conclusion

We have shown that the inactivation peptide of Kv1.4 exerts significant effects on the C-type–inactivated Na^+ tail currents of Kv1.4 and Kv1.5, including slowing of tail current kinetics, and a reduction in peak tail current magnitude. These effects are observed whether the inactivation peptide binds to open channels or to C-type–inactivated channels, suggesting that the inner vestibule of Kv channels is cytosolically accessible before, and after, the onset of C-type inactivation. Kinetic modeling suggests that the inactivation peptide binds stably to the pore of C-type–inactivated channels, delaying transitions through Na^+-permeable states traversed during recovery from inactivation.

We are very grateful to Dr. S.J. Kehl for his careful reading and frequent discussion of the manuscript. We thank Anu Khurana for preparation of cells, and Woo Sung Choi for assistance with experiments.

This work was supported by operating grants to D. Fedida from the CIHR and the Heart and Stroke Foundation of B.C. & Yukon. H. Kurata is supported by a CIHR predoctoral fellowship and a Michael Smith Foundation for Health Research incentive award.

Olaf S. Andersen served as editor.

Submitted: 30 September 2003
Accepted: 3 March 2004

REFERENCES

Baukrowitz, T., and G. Yellen. 1995. Modulation of K^+ current by frequency and external $[K^+]$: A tale of two inactivation mechanisms. *Neuron.* 15:951–960.

Baukrowitz, T., and G. Yellen. 1996. Use-dependent blockers and exit rate of the last ion from the multi-ion pore of a K^+ channel. *Science.* 271:653–656.

Bezanilla, F., E. Perozo, D.M. Papazian, and E. Stefani. 1991. Molecular basis of gating charge immobilization in Shaker potassium channels. *Science.* 254:679–683.

Castle, N.A., S.R. Fadous, D.E. Logothetis, and G.K. Wang. 1994. 4-aminopyridine binding and slow inactivation are mutually exclusive in rat Kv1.1 and *Shaker* potassium channels. *Mol. Pharmacol.* 46:1175–1181.

Choi, K.L., R.W. Aldrich, and G. Yellen. 1991. Tetraethylammonium blockade distinguishes two inactivation mechanisms in voltage-activated K^+ channels. *Proc. Natl. Acad. Sci. USA.* 88:5092–5095.

Choi, K.L., C. Mossman, J. Aubé, and G. Yellen. 1993. The internal quaternary ammonium receptor site of *Shaker* potassium channels. *Neuron.* 10:533–541.

Demo, S.D., and G. Yellen. 1991. The inactivation gate of the *Shaker* K^+ channel behaves like an open-channel blocker. *Neuron.* 7:743–753.

Fedida, D., N.D. Maruoka, and S. Lin. 1999. Modulation of slow inactivation in human cardiac Kv1.5 channels by extra- and intracellular permeant cations. *J. Physiol.* 515:315–329.

Ficker, E., W. Jarolimek, J. Kiehn, A. Baumann, and A.M. Brown. 1998. Molecular determinants of dofetilide block of HERG K^+ channels. *Circ. Res.* 82:386–395.

Hoshi, T., W.N. Zagotta, and R.W. Aldrich. 1990. Biophysical and molecular mechanisms of *Shaker* potassium channel inactivation. *Science.* 250:533–538.

Hoshi, T., W.N. Zagotta, and R.W. Aldrich. 1991. Two types of inactivation in *Shaker* K^+ channels: Effects of alterations in the carboxy-terminal region. *Neuron.* 7:547–556.

Jiang, X., G.C. Bett, X. Li, V.E. Bondarenko, and R.L. Rasmusson. 2003a. C-type inactivation involves a significant decrease in the intracellular aqueous pore volume of Kv1.4 K^+ channels expressed in *Xenopus* oocytes. *J. Physiol.* 549:683–695.

Jiang, Y., A. Lee, J. Chen, V. Ruta, M. Cadene, B.T. Chait, and R.

MacKinnon. 2003b. X-ray structure of a voltage-dependent K^+ channel. *Nature.* 423:33–41.

Kiss, L., J. LoTurco, and S.J. Korn. 1999. Contribution of the selectivity filter to inactivation in potassium channels. *Biophys. J.* 76: 253–263.

Kurata, H.T., G.S. Soon, and D. Fedida. 2001. Altered state dependence of C-type inactivation in the long and short forms of human Kv1.5. *J. Gen. Physiol.* 118:315–332.

Liu, Y., M.E. Jurman, and G. Yellen. 1996. Dynamic rearrangement of the outer mouth of a K^+ channel during gating. *Neuron.* 16: 859–867.

Loots, E., and E.Y. Isacoff. 1998. Protein rearrangements underlying slow inactivation of the *Shaker* K^+ channel. *J. Gen. Physiol.* 112: 377–389.

Lopez-Barneo, J., T. Hoshi, S.H. Heinemann, and R.W. Aldrich. 1993. Effects of external cations and mutations in the pore region on C-type inactivation of Shaker potassium channels. *Receptors Channels.* 1:61–71.

MacKinnon, R., R.W. Aldrich, and A.W. Lee. 1993. Functional stoichiometry of Shaker potassium channel inactivation. *Science.* 262: 757–759.

Morales, M.J., J.O. Wee, S. Wang, H.C. Strauss, and R.L. Rasmusson. 1996. The N-terminal domain of a K^+ channel beta subunit increases the rate of C-type inactivation from the cytoplasmic side of the channel. *Proc. Natl. Acad. Sci. USA.* 93:15119–15123.

Ogielska, E.M., W.N. Zagotta, T. Hoshi, S.H. Heinemann, J. Haab, and R.W. Aldrich. 1995. Cooperative subunit interactions in C-type inactivation of K channels. *Biophys. J.* 69:2449–2457.

Panyi, G., Z. Sheng, L. Tu, and C. Deutsch. 1995. C-type inactivation of a voltage-gated K^+ channel occurs by a cooperative mechanism. *Biophys. J.* 69:896–903.

Pardo, L.A., S.H. Heinemann, H. Terlau, U. Ludewig, C. Lorra, O. Pongs, and W. Stühmer. 1992. Extracellular K^+ specifically modulates a rat brain K^+ channel. *Proc. Natl. Acad. Sci. USA.* 89:2466–2470.

Rasmusson, R.L., M.J. Morales, R.C. Castellino, Y. Zhang, D.L. Campbell, and H.C. Strauss. 1995. C-type inactivation controls recovery in a fast inactivating cardiac K^+ channel (Kv1.4) expressed in *Xenopus* oocytes. *J. Physiol.* 489:709–721.

Rasmusson, R.L., M.J. Morales, S. Wang, S. Liu, D.L. Campbell, M.V. Brahmajothi, and H.C. Strauss. 1998. Inactivation of voltage-gated cardiac K^+ channels. *Circ. Res.* 82:739–750.

Roux, M.J., R. Olcese, L. Toro, F. Bezanilla, and E. Stefani. 1998. Fast inactivation in *Shaker* K^+ channels. Properties of ionic and gating currents. *J. Gen. Physiol.* 111:625–638.

Ruppersberg, J.P., R. Frank, O. Pongs, and M. Stocker. 1991. Cloned neuronal $I_K(A)$ channels reopen during recovery from inactivation. *Nature.* 353:657–660.

Starkus, J.G., L. Kuschel, M.D. Rayner, and S.H. Heinemann. 1997. Ion conduction through C-type inactivated *Shaker* channels. *J. Gen. Physiol.* 110:539–550.

Starkus, J.G., L. Kuschel, M.D. Rayner, and S.H. Heinemann. 1998. Macroscopic Na^+ currents in the "nonconducting" *Shaker* potassium channel mutant W434F. *J. Gen. Physiol.* 112:85–93.

Starkus, J.G., Z. Varga, R. Schonherr, and S.H. Heinemann. 2003. Mechanisms of the inhibition of Shaker potassium channels by protons. *Pflugers Arch.* 447:44–54.

Wang, S., M.J. Morales, S. Liu, H.C. Strauss, and R.L. Rasmusson. 1997a. Modulation of HERG affinity for E-4031 by $[K^+]o$ and C-type inactivation. *FEBS Lett.* 417:43–47.

Wang, S.M., S.G. Liu, M.J. Morales, H.C. Strauss, and R.L. Rasmusson. 1997b. A quantitative analysis of the activation and inactivation kinetics of *HERG* expressed in *Xenopus* oocytes. *J. Physiol.* 502:45–60.

Wang, Z.R., and D. Fedida. 2002. Uncoupling of gating charge movement and closure of the ion pore during recovery from inactivation in the Kv1.5 channel. *J. Gen. Physiol.* 120:249–260.

Wang, Z.R., J.C. Hesketh, and D. Fedida. 2000. A high-Na^+ conduction state during recovery from inactivation in the K^+ channel Kv1.5. *Biophys. J.* 79:2416–2433.

Wissmann, R., W. Bildl, D. Oliver, M. Beyermann, H.R. Kalbitzer, D. Bentrop, and B. Fakler. 2003. Solution structure and function of the "tandem inactivation domain" of the neuronal A-type potassium channel Kv1.4. *J. Biol. Chem.* 278:16142–16150.

Yellen, G., D. Sodickson, T.-Y. Chen, and M.E. Jurman. 1994. An engineered cysteine in the external mouth of a K^+ channel allows inactivation to be modulated by metal binding. *Biophys. J.* 66: 1068–1075.

Zhang, S., H.T. Kurata, S.J. Kehl, and D. Fedida. 2003. Rapid induction of P/C-type inactivation is the mechanism for acid-induced K^+ current inhibition. *J. Gen. Physiol.* 121:215–225.

Zhou, M., J.H. Morais-Cabral, S. Mann, and R. MacKinnon. 2001. Potassium channel receptor site for the inactivation gate and quaternary amine inhibitors. *Nature.* 411:657–661.